Contribution on transient flow modelling in storm sewers

Contribution sur la modélisation de l'écoulement transitoire dans les collecteurs

MUSANDJI FUAMBA, *Research Associate, Hydrodynamic Laboratory, Polytechnic School of Montreal, C.P. 6079, succ. Centre-ville, Montreal (Quebec) Canada H3C 3A7*

ABSTRACT

Currently, the Preissmann slot model still enjoys popularity in modelling the transition between free-surface and fully pressurised flows in tail-race tunnels. However a fully dynamic and transient modelling technique is needed to predict the surge front location and velocity, the pressure rise in the full flow zone and the water depth change in the free-surface zone. In this paper, the transient flow is modelled and only one surge front is considered. Three 1-D models, which differ from each other by the computational method used to calculate either the free-surface or the full flow conditions, have been developed and applied successfully to both laboratory and field data. Predictions have been compared to measurements and good agreement found. Comparison between the three fully dynamic models was done and selective criteria were forwarded.

RESUME

Le modèle Preissmann continue d'être utilisé dans le calcul de l'écoulement transitoire survenant lorsqu'un écoulement à surface libre se transforme en écoulement en charge. Cependant il est nécessaire de prédire la position ainsi que la vitesse de l'onde de remplissage avec un modèle transitoire entièrement dynamique. L'écoulement transitoire a été modélisé en une dimension dans cet article et trois variantes de cette modélisation – différente l'une de l'autre par la méthode de calcul utilisée pour calculer les conditions de l'écoulement dans les zones à surface libre et en charge- sont décrites et appliquées à des données à la fois de laboratoire et de prototype. Les critères de sélection de l'une ou l'autre des variantes ont été fixés à l'issue d'une étude comparative effectuée entre ces trois modèles. La comparaison entre les valeurs calculées et celles mesurées de pression a montré une réelle concordance.

Introduction

The purpose of storm sewer design is simple: to convey water under free-surface conditions. The classification of the flow in a sewer pipe, however, is more complicated. Yen (1986) divides this flow into three sections: the entrance, the pipe flow and the exit. He describes four cases of entrance conditions and four more cases of exit conditions.

One case of the latter is when the pipe flow is under downstream control after a violent storm. The water depth then increases quickly and flow may remain of the free-surface type: this is phase 1. However, when the water surface reaches the sewer invert at a junction or the downstream end, a surge front develops and propagates towards the boundary at the other end. The downstream zone behind the surge becomes more and more elongated while the piezometric head rises gradually. The transient flow is highly dynamic: this is phase 2 where free-surface and pressurised zones exist simultaneously and where the sewer system is subjected to positive and negative pressures.

Once the surge front reaches the opposite end-boundary, the flow is pressurised everywhere; this is phase 3, also a very dynamic phase. The pressure rise produced at the end of phase 2 may result in overflow at street level outlets. When the runoff diminishes, overflow stops and the sewer system starts losing water. The free-surface flow zone is re-established near the upstream end and gradually spreads to the entire system which is phase 4.

Because of the complexity of the transient flow, it appears necessary to handle combined free-surface-pressurised flows by the use of an efficient, fully dynamic model able to simulate the surge front propagation, take into account as well as provide the negative pressures and incorporate the interaction between the surge front and internal/external boundaries.

State of the art

The first well-known investigation of a transient flow where flow conditions may change from free-surface to pressurised, and vice versa, was of the Limmatwerk Wettingen tail-race tunnel (Meyer-Peter and Favre 1932). Cunge and Wegner (1966) described an implicit finite-difference scheme that they applied to the Wettingen system. They studied the pressurised flow in the tunnel as if it were a free-surface flow by assuming a narrow slot to exist in the upper part of the tunnel, the width of the slot being calculated to provide the correct sonic speed. This approach has been credited to Preissmann. Later, Cunge (1966) conducted a study of translation waves in a power canal containing a series of transitions, including a siphon. Pseudo-viscosity methods were employed to describe the movement of bores in open-channel reaches.

Wiggert (1972) studied the transient flow phenomena and his analytical considerations included open-channel surge equations that were solved by the method of characteristics. He subjected it to subcritical flow conditions and used Meyer-Peter and Favre's description of the surge wave in the tunnel (under subcritical flow conditions). His solution resulted from applying a similarity between the movement of a hydraulic bore and an interface (that is, a surge front wave). Following Wiggert's model, Song, Cardle and Leung (1983) developed two mathematical models of unsteady free-surface/pressurised flows using the method of characteristics (specified time and space) to compute flow conditions in

Revision received May 8, 2002. Open for discussion till April 30, 2003.

two flow zones. They showed that the pressurised phenomenon is a dynamic shock requiring a full dynamic treatment even if inflows and other boundary conditions change very slowly. However, the Song models do not include the bore presence in the free-surface zone.

McCorquodale and Hamam (1983) proposed a rigid water column approach to model the mixed flow pressure transients. This model assumes a hypothetical stationary bubble across compression and expansion processes. Li and McCorquodale (1999) extended the rigid water column approach to allow for the transport of the trapped air bubble.

Jun (1985) conducted a study to compare the two methods of mathematical simulation for pressurised flow in sewer networks: his so-called standard technique and the Preissmann slot technique. The first technique keeps track of the sewers that are being pressurised, treating them as a single flow reach where the discharge is assumed to be the same throughout the entire length of the single flow reach (incompressible fluid). The second technique treats the pressurised flow as open-channel flow by using a hypothetical narrow, open slot at the invert of the pipe. However, verification of assumptions used in the developed simulation models was not done by the use of reliable field and/or laboratory data. Some high flows where peak discharge is reached quickly cannot be solved efficiently without using a totally dynamic model where the fluid is assumed compressible.

In the last few years, numerical models mainly based on the Preissmann slot technique have been developed to handle the flow transition in sewer systems, the most popular being Mouse, HydroWorks and Canoe. Pressurised flow computations in the Mouse model are facilitated through implementation of a narrow slot as a vertical extension of the closed pipe cross-section. Free surface and pressurised flows are thus described within the same basic algorithm, which ensures a smooth and stable transition in all situations (Mouse 2000). HydroWorks uses the conduit or the pressurised pipe models for the selected surcharged pipes. The conduit model uses the Preissmann slot technique to solve the Saint-Venant equations. The pressurised pipe model assumes an incompressible fluid which means a constant discharge through the pipe (HydroWorks 2000). Canoe, an amalgamation of the French models Cedre and Caredas, also makes use of the Preissmann slot technique when pipes become pressurised (Canoe 1999). So does Rio, a sewer system analysis computer program developed by the Hydraulic Laboratory of Catholic University of Leuven in Belgium (Rio 1993) to predict unsteady flow conditions in sewer systems.

Implementing the Preissmann slot technique has the advantage of using only one flow type (free-surface flow) throughout the whole sewer system and of being able to easily quantify the pressure head when pipes pressurise. However, this technique neglects the resulting dynamic wave phenomena and fails to accurately show how the pressurised zone can influence the free-surface zone (Canoe 1999). The pressurised pipe model can be used to overcome these limitations.

In special cases where flows vary rapidly it would be interesting to consider the sewer network as a distributed system where the transient phenomenon occurs in the form of a travelling wave with a compressible fluid. The model described in this paper does that. This model considers only one surge front and does not incorporate the air bubbles and the interfacial instability phenomenon because these issues are too complex and difficult to be accurately studied at the present time. Moreover, the fully dynamic model developed here successfully solves the transition problem in phases 2 and 4, whether or not the free-surface flow is of the subcritical or the supercritical type. If appropriate, a hydraulic jump in the free-surface flow is also predicted. The three modelling variants called Traflo1, Traflo2 and Traflo3 incorporate enough of the dynamic behaviour of the transient phenomenon into the numerical formulation to provide insight into the different computational methods which may be used to compute the flow conditions in all zones. Traflo1 and Traflo2 use the pressurised pipe model whereas Traflo3 makes the assumption of a compressible fluid.

Numerical modelling

Model 1: Traflo1

As stated earlier, the transition process starts with phase 1, with free-surface flow throughout the sewer system. We assume that the water depth is increasing faster at the upstream boundary. If the characteristics grid scheme of the method of characteristics is used to second order approximation of finite differences to compute the flow conditions at location P, in the x-t plane, the simplified de St. Venant equations may be written as (Chaudhry 1993, Roberson et al. 1998)

$$g\frac{\partial y}{\partial x}+V\frac{\partial V}{\partial x}+\frac{\partial V}{\partial t}+g(S-S_0)=0 \tag{1}$$

$$\frac{A}{B}\frac{\partial V}{\partial x}+V\frac{\partial y}{\partial x}+\frac{\partial y}{\partial t}=0 \tag{2}$$

which have the following solution

$$V_P=C_1+C_2y_P \tag{3}$$

$$V_P=C_3-C_4y_P \tag{4}$$

where g is the acceleration due to gravity, y the water depth, V the mean cross-sectional velocity, A the wetted cross-sectional area, B the water surface width, x the distance along the sewer, t the time, S_0 the sewer bottom slope and S the friction slope. C_1, C_2, C_3 and C_4 are expressed as

$$C_4 = g\ (\ 1/c_R + 1/c_P\ );$$
$$C_3 = V_R + C_4y_R - g\ (\ S_R + S_P - 2S_0)(\ t_P - t_R\ )/2$$
$$C_2 = g\ (\ 1/c_S + 1/c_P\ );$$
$$C_1 = V_S - C_2y_S - g\ (\ S_S + S_P - 2S_0)(\ t_P - t_S\ )/2$$

where c is the gravity wave celerity. Subscripts R and S are locations defining, respectively, positive and negative characteristic lines drawn from P.

Free-surface computations are performed in the streamwise direction until the water surface reaches the sewer invert at the upstream boundary. Then a surge front develops at the upstream end. While propagating, this surge appears like an interface whose shape is not regular (Fuamba 1996) and which separates the developing full flow from the initially free-surface flow. Following the numerical scheme of Wiggert (1972) and using the Shock Fitting Method (Cunge et al. 1980), the transient flow may be modelled by expressing the interface (front surge) continuity and momentum conservation. In fact, this interface behaves as a moving internal boundary condition. Computed flow conditions at this discontinuity are therefore considered as downstream boundary conditions for the full flow zone and as upstream boundary conditions for the free-surface zone.
An inventory of unknowns includes the surge front location x_1 and velocity w defined below, time t, velocity V_1 and pressure head h_1 upstream of the interface; the velocity V_2 and water depth y_2 downstream of the interface. Seven equations are thus needed to solve for the seven unknowns. The first two equations are Eqs. 3 and 4, which may be differently written as

$$\frac{g}{2}\left(\frac{1}{c_R}+\frac{1}{c_P}\right)(y_P - y_R)+V_P-V_R + \frac{g}{2}(S_R+S_P-2S_0)(t_P-t_R)=0 \tag{5}$$

$$-\frac{g}{2}\left(\frac{1}{c_S}+\frac{1}{c_P}\right)(y_P - y_S)+V_P-V_S + \frac{g}{2}(S_S+S_P-2S_0)(t_P-t_S)=0 \tag{6}$$

The third equation is for the negative characteristic C^-.

$$x_P - x_S - \left(\frac{V_P+V_S}{2}-\frac{c_P+c_S}{2}\right)(t_P-t_S)=0 \tag{7}$$

The next two equations are, respectively, the continuity and momentum equations at the interface

$$A_1(V_1-w)=A_2(V_2-w) \tag{8}$$

$$g(A_2\overline{y_2}-A_1h_1)=A_1(V_1-w)(V_1-V_2) \tag{9}$$

where w is the interface (surge front) propagation velocity and $\boldsymbol{y}$ is the distance from the free-surface to the centroid of the wetted cross-section. The momentum balance formulated for the full flow zone of length x_1 from a given upstream location 0 (where the pressure head is known) to location 1 immediately behind (upstream) the interface may be expressed by

$$x_S\frac{dV_1}{dt}=g(h_0-h_1)+gx_1(S_0-S)=0 \tag{10}$$

Let us now assume that the surge front velocity is described by

$$\frac{dx_1}{dt}=w \tag{11}$$

According to Figure 1 and from the previous computational step, the flow conditions t, x_1, V_1, h_1, V_2, y_2, w at position B and x, t, V, y at R and S are considered known. Computation at the surge front follows an iterative procedure until convergence is reached. The Runge-Kutta technique is used to obtain the solution to Eq. (10). During phase 3, the sewer system is pressurised along its entire length L. If h_0 and h_1, respectively, are the pressure heads at the upstream and downstream ends, then Eq. (10) becomes

$$L\frac{dV_1}{dt}=g(h_0-h_1)+gL(S_0-S)=0 \tag{12}$$

and the Runge-Kutta technique may also be applied here.

Model 2: Traflo2

Flow conditions in the free-surface zone are solved by using the specified characteristics scheme and first-order integration (Chaudhry 1993). Satisfying the Courant stability condition $\Delta t = \Delta x / |V| + c$, y_P and V_P are

$$y_P=\frac{1}{c_R+c_S}\left(y_S c_R + y_R c_S + c_R c_S\left(\frac{V_R-V_S}{g}-\Delta t(S_R-S_S)\right)\right) \tag{13}$$

$$V_P = V_R - g\frac{y_P-y_R}{c_R}-g\Delta t(S_R-S_0) \tag{14}$$

where values at R and S are obtained by linear interpolation. Six unknowns x_1, V_1, h_1, V_2, y_2 and w define the flow conditions at the interface which has moved from B to P in Figure 2. The six needed equations are Eqs. (13) and (14) for open-channel flow, the continuity and momentum equations (Eqs. 8 and 9), the mo-

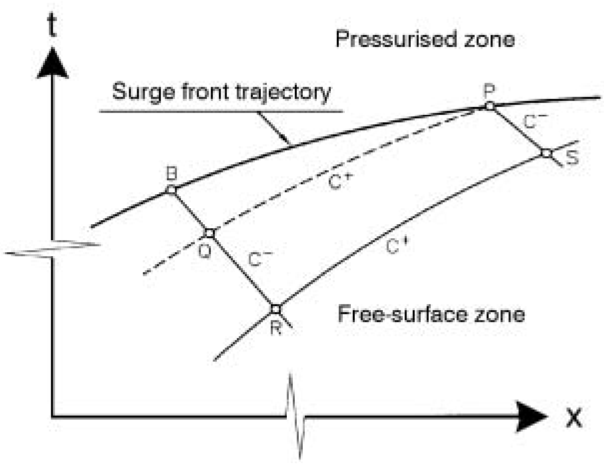

Fig. 1. Surge Front Propagation, Traflo 1.

mentum balance equation (Eq. 10) and the surge front propagation (Eq. 11).

V_{R2}, c_{R2}, y_{R2} may be obtained using linear interpolation between B and M from Figure 2 as follows

$$V_{R2} = \frac{V_M - \alpha_1 (V_M c_2 - c_M V_2)}{1 + \alpha_1 (V_M - V_2 + c_M - c_2)} \tag{15}$$

$$c_{R2} = \frac{c_M - \alpha_1 (c_M - c_2) V_{R2}}{1 + \alpha_1 (c_M - c_2)} \tag{16}$$

where $V_M = V_C - (x_C - x_P)(V_C - V_2)/(x_C - x_B)$; $\alpha_1 = \Delta t/(x_P - x_B)$ and $y_M = y_C - (x_C - x_P)(y_C - y_2)/(x_C - x_B)$.

The term y_{R2} may be computed from the following equation

$$y_{R2} = y_M - \alpha_1 (V_{R2} + c_{R2})(y_M - y_2) \tag{17}$$

If the free-surface flow is subcritical, C_2^- passes by S_2 and then V_{S2}, c_{S2}, y_{S2} may be found by linear interpolation between C and M from Figure 2 as

$$V_{S2} = \frac{V_M - \alpha_2 (V_M c_C - c_M V_C)}{1 - \alpha_2 (V_M - V_C + c_C - c_M)} \tag{18}$$

$$c_{S2} = \frac{c_M + \alpha_2 (c_M - c_C) V_{S2}}{1 + \alpha_2 (c_M - c_C)} \tag{19}$$

where $\alpha_2 = \Delta t/(x_C - x_P)$.

The term y_{S2} may be found from the following equation

$$y_{S2} = y_M + \alpha_2 (V_{S2} - c_{S2})(y_M - y_C) \tag{20}$$

If the flow is supercritical, then C_2^- passes by $S'2$ and then $V_S{'}_2$, $c_S{'}_2$, $y_S{'}_2$ may be found by linear interpolation between C and M as

$$V_{S'2} = \frac{V_M + \alpha_1 (V_M c_2 - c_M V_2)}{1 + \alpha_1 (V_M - V_2 - c_M + c_2)} \tag{21}$$

$$c_{S'2} = \frac{c_M - \alpha_1 (c_M - c_2) V_{S'2}}{1 - \alpha_1 (c_M - c_2)} \tag{22}$$

The term $y_S{'}_2$ may be obtained from

$$y_{S'2} = y_M - \alpha_1 (V_{S'2} - c_{S'2})(y_M - y_2) \tag{23}$$

Computation at the surge front is performed following this procedure. At each time step, one assumes initial values at point P, for example $x_P = x_B$; $V_{1P} = V_1$; $w_P = w$. Then the surge front may be located using Eq. (11) which may be written in the form

$$x_{1P} = x_B + w\Delta t \tag{24}$$

Afterwards, V'_{2P} et y'_{2P} may be computed depending on the flow regime (subcritical or supercritical). V'_{1P} and w'_P may be calculated from

$$\frac{dV'_{1P}}{dt} = \frac{1}{x'_{1P}} \frac{(V'_{1P} - V'_{2P})^2}{(1 - A_1 / A'_{2P})} + \frac{g}{x'_{1P}} (h_0 - \frac{A'_{2P}}{A_1} \overline{y'_{2P}}) + g(S_0 - S) \tag{25}$$

obtained by combining Eqs. (8), (9) and (10) and substitution of h_1. The Runge-Kutta method may be used to solve for V'_{1P} from Eq. (25). Computations continue iteratively until convergence is reached. Finally all six unknowns are found at each step. The same computational procedure is available for a downstream starting surge front except that w is taken positive in the $-x$ direction for computational convenience. Consequently, w is considered negative in the relevant equations.

When the free-surface conditions are such that a bore occurs, the Shock Fitting Method is used to isolate the discontinuity and to compute upstream and downstream flow conditions. The previously described computational procedure may then be implemented.

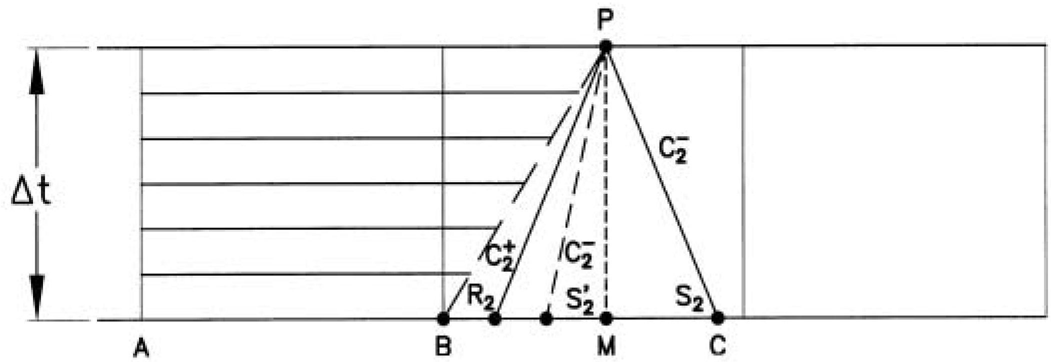

Fig. 2. Surge Front Propagation, Traflo 2.

Model 3: Traflo3

Following the two models of Song et al. (1983), the specified characteristics method is used to predict flow conditions in the closed conduit zone as well as in the free-surface zone. Eqs. 13 and 14 are necessary to solve for the free-surface conditions in phases 1 and 2. Considering a compressible fluid here, flow conditions at the interface (see Figure 3) require solution for the six unknowns x_1, V_1, h_1, V_2, y_2 and w. The six equations required for the solution are: the two open-channel flow (Eqs. 13 and 14), the continuity and momentum equations (Eqs. 8 and 9) at the interface, the surge front propagation (Eq. 11) and one of the two characteristic equations in the pressurised zone. If the surge front is moving downstream and because an equivalent stationary hydraulic jump must occur from a supercritical to a subcritical condition according to Song et al., the required condition reads

$$a + V_1 > w > c_2 + V_2 \tag{26}$$

where a is the waterhammer celerity. The positive characteristic equation C_1^+ is the only required. If the surge front is propagating upstream, the required condition

$$a - V_1 > w > c_2 - V_2 \tag{27}$$

makes use of the equation for the negative characteristic C_1^- to close the problem.

The Courant stability condition has to be satisfied both in the free-surface and the full flow zones, where the time steps, respectively, Δt and $\Delta t'$ should be fixed such that $\Delta t' = \Delta t/n$. Computations performed by the author have shown that reliable results are obtained for $150 \le n \ge 250$. Flow at R_1 is found from flow at A' and B'.This procedure increases the number of computations principally by the iterative process. Pressurised flow behind the surge front is computed by using the method of characteristics to solve the equations describing the transient-state flow in closed conduits (Chaudhry 1987, Streeter and Wylie 1981) whereas free surface flow upstream of the surge is calculated by using the method of characteristics.

Calculations during phase 4 are performed by using the two open-channel flow (Eqs. 13 and 14), the continuity and momentum equations (Eqs. 8 and 9) at the interface, the surge front propagation (Eq. 11) and finally the energy equation defined by Whitham

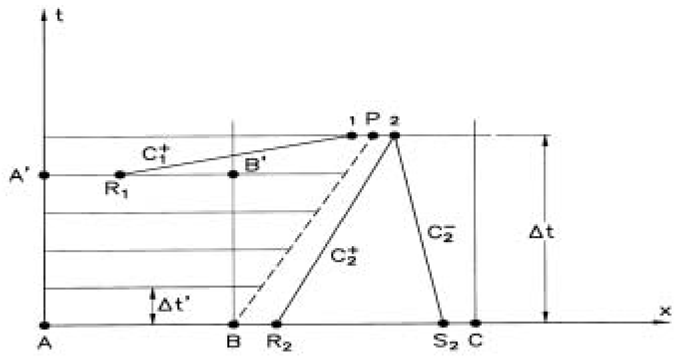

Fig. 3. Surge Front Propagation, Traflo 3.

(1973) for a moving discontinuity (i.e. a surge front) in a flowing fluid

$$\frac{(V_2 + w)^2}{2g} + y_2 = \frac{(V_1 + w)^2}{2g} + h_1 + h_L \tag{28}$$

where subscripts 1 and 2 refer respectively to the pressurised and free-surface zones and h_L is the energy head lost to be estimated from experiments.

Table 1 summarizes the selective criteria for the different Traflos models. Depending on the flow type or changes in flow, selection of the appropriate Traflo variant is made.

Table 1. Selective criteria for Traflo1, Traflo2 and Traflo3

	Traflo1	*Traflo2*	*Traflo3*
Simple system	X	X	X
Supercritical flow	-	X	X
Bore presence	-	X	X
Flow varying rapidly	-	-	X

Traflos application

Case Study No1

To illustrate Traflos application, 2 numerical examples are studied in the present paper. The first case is an experimental case where laboratory data were collected. As shown in Figure 4, an upstream reservoir was supplied by a large head tank by means of a control valve to maintain flow in a 6-meter long PVC pipe of 100 mm diameter D. A sliding weir was operated downstream to control the downstream water depth z_1 in such a way that

$$Q_{out} = c_d \sqrt{2g(z_1 - h_0^*)}(z_1 - h_0^*)B_r \tag{29}$$

where the weir height was $h_0^* = 8.5$ cm; the discharge coefficient $c_d = 0.48$ and the weir width $B_r = 65$ cm. z_1 is the downstream water depth and Q_{out} the inflow discharge.

Starting from complete rest (initial condition), the control valve was gradually opened. Then, water depth at the upstream end increased until the pipe invert was reached as shown in Figure 4. The pipe became initially submerged at the upstream cross-section. A surge front then formed and started propagating downstream, forming pressurised flow behind. Once the surge arrived at the downstream end, full flow occurred in the entire pipe. Pressure measurements were made at selected locations specified also in Figure 4 by means of pressure transducers, and compared to predicted values.

The appropriate friction formula used for the pipe flow was $1/f^{0.5} = -2\log_{10}[2.51/Ref^{0.5} + 3.10^{-3}/10.7D]$ where Re is the Reynolds number (Fuamba 1997). The slope was $S_0 = 0.0013$. A Courant number of value 0.9 was adopted in all Traflos simulations to maintain stable the numerical scheme, in order to make reliable

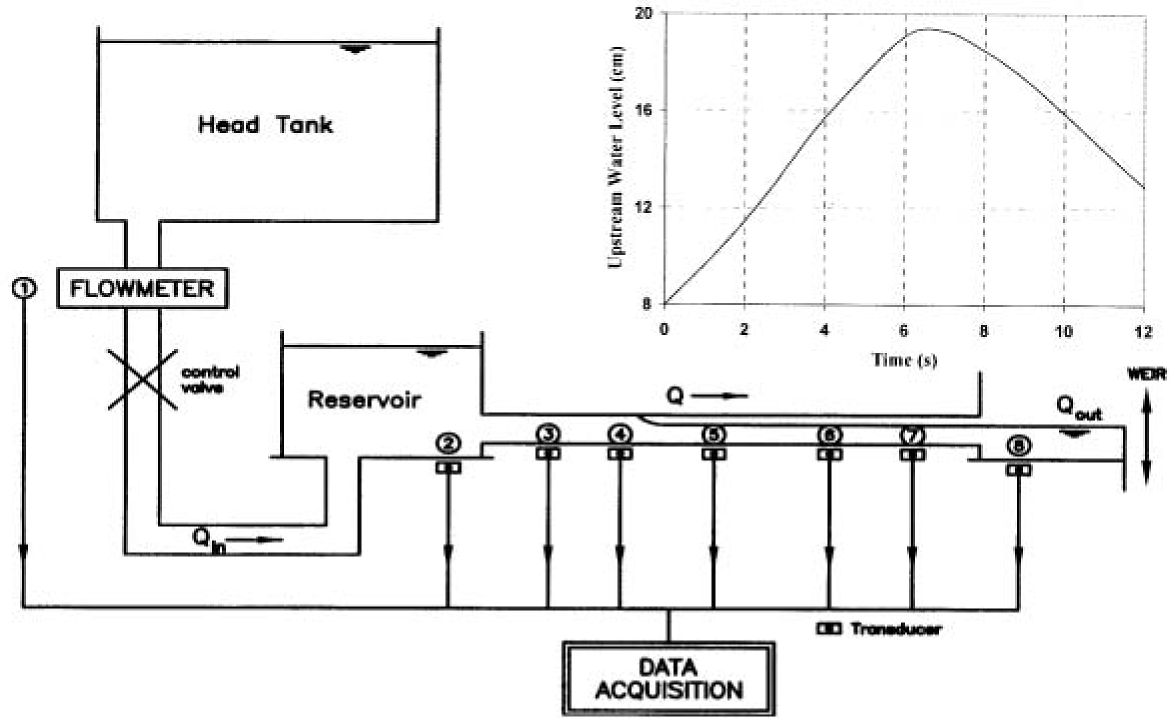

Fig. 4. Case Study 1 Setup.

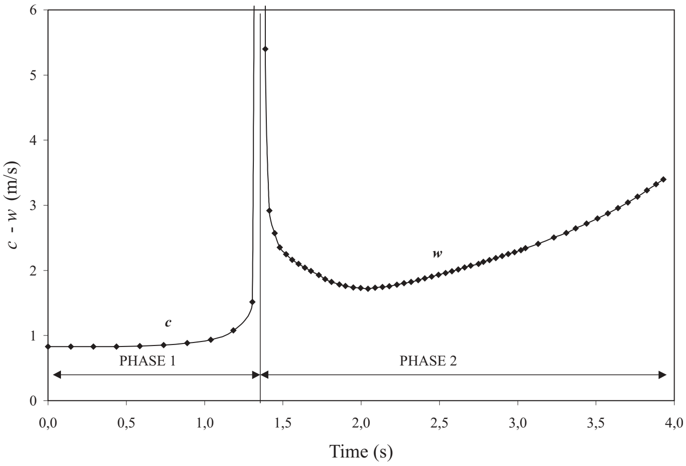

Fig. 5. c and w Variation, Case Study 1, Traflo 1.

predictions. So, Δx=0.30m and Δt=0.09s for c_{max}=2m/s and V_{max}=1m/s. If n=200, $\Delta t'$=0.00045 s. The estimated value of the waterhammer celerity was a=575m/s.

The Traflo1 simulation revealed that c values remained less than 1 m/s for times inferior to 1s (Figure 5). The surge front formed at 1.348 s and phase 2 lasted 2.58 s. Figure 6 shows a comparison between pressure predictions and measurements at location 5 (2.50 m from the upstream end). One can easily distinguish when the surge front reached location 5. At this time, location 5 recorded its largest value; pressure suddenly increased from 37 to 43 cm before continuing to increase gradually. Predictions are quite similar to laboratory measurements, as indicated in Figure 6.

Unlike Traflo1, Traflo2 at each time step illustrates the free-surface profile upstream of the interface during the transient phase. Figure 7 shows how fast the velocity of the surge front really is:

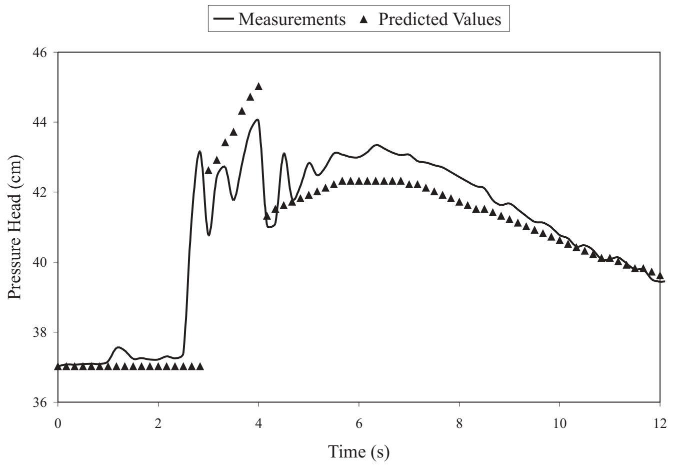

Fig. 6. Comparison Predicted/Measured Prtessure Values at Location 5, Traflo 1.

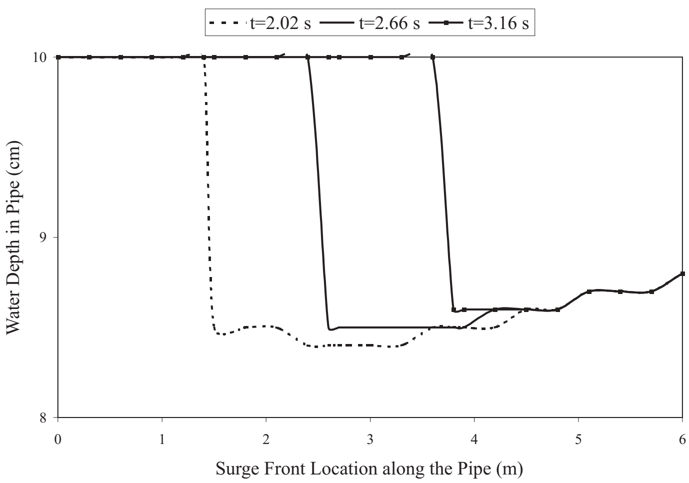

Fig. 7. Successive Surge Front Locations, Traflo 2.

2.02 s after the start of the flow, the surge front already travelled 1.50 m and at time 3.16 s, it passed location 3.84 m. This means that in only 1.1 s, a 2 m length from the upstream end of pipe got pressurised.

Traflo3 computations took significantly more time. Due to its modelling in phases 2 and 3 where $\Delta t'$ was used, Traflo3 required 52.5 times more than Traflo1 and 26 times more than Traflo2 when the results predicted by the three variants are close to each other. When normalizing pressure measurements at location 3 (0.50 m from the upstream end) as unity, predicted pressures relative to location 3 are compared in Figure 8. Then the predicted behavior (trend) of all variants is similar during the transient phase. Slight differences are noted during phase 3 and the Traflo1 results appeared to be closest to the measurements. Nevertheless, the relative error between measurements and predictions do not exceed 2% for the entire simulation.

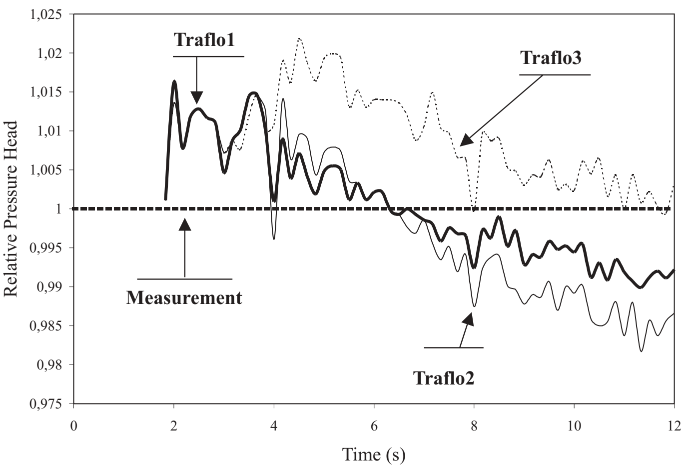

Fig. 8. Comparison of Relative Pressure Heads at Location 3.

Case Study No 2

The second case study is a practical case formed by three sewers, as shown in Figure 9. A storm discharge of 111 l/s occurring during 15 min. resulted in a rapid rise of water depth at section 1 (Figure 10) until a surge front started propagating towards section 3. The Manning coefficient used was n=0.013. Satisfying the Courant number of 0.9, Δx=5m and Δt=0.8s. The estimated value of the waterhammer celerity was 628 m/s.

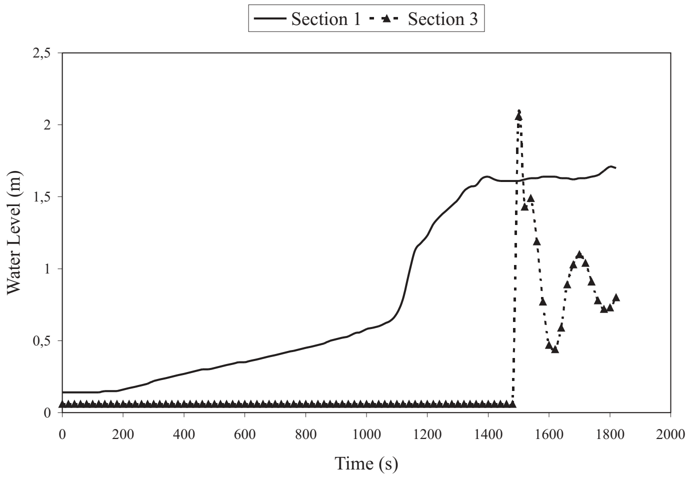

Fig. 10. Water Depth Variation at Sections 1 and 3.

Rio (1993) was used here to compare with Traflos' results. The wave celerity is determined from the standard wave celerity equation for free-surface flow c $(=g[A/B]^{1/2}$ where B is the free-surface width and A the cross sectional area) and the surge velocity is known once the elasticity is fixed for both sewer pipe and water. In the slot simulation, the wave celerity clearly depends on the slot width.

Comparison between Rio and Traflo2 pressure values predicted at section 3 (Figure 11) showed that Rio values are relatively late (delay of 4.20 min.). The peak value of 18 kPa was found when the surge front arrived at section 3 at time 25 min., according to Traflo2. Comparison mainly indicates the advantages of using a fully dynamic and transient model. Not only is the surge front location and propagation accurately predicted during the transient flow phase, but realistic head loss coefficients are used to simulate the flow conditions.

Conclusions and recommendations

A fully dynamic model describing the transition between free-surface and pressurised flows has been developed with three vari-

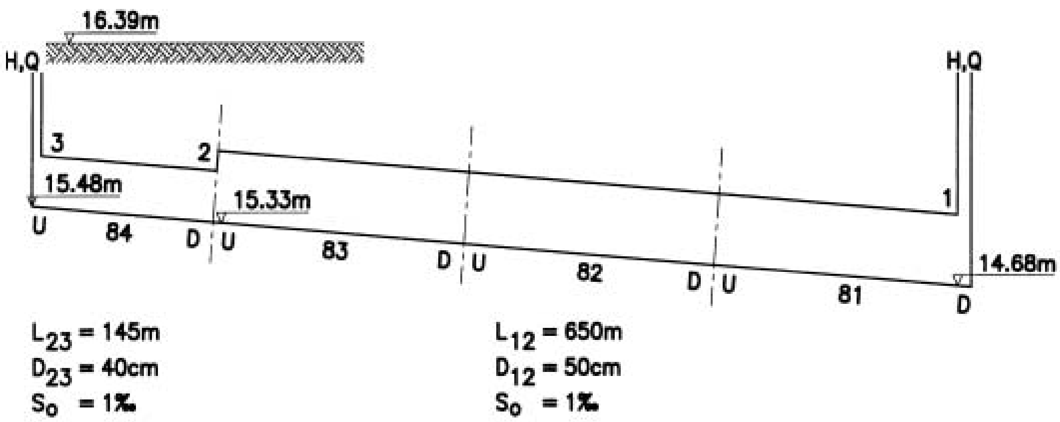

Fig. 9. Case Study 2 Setup.

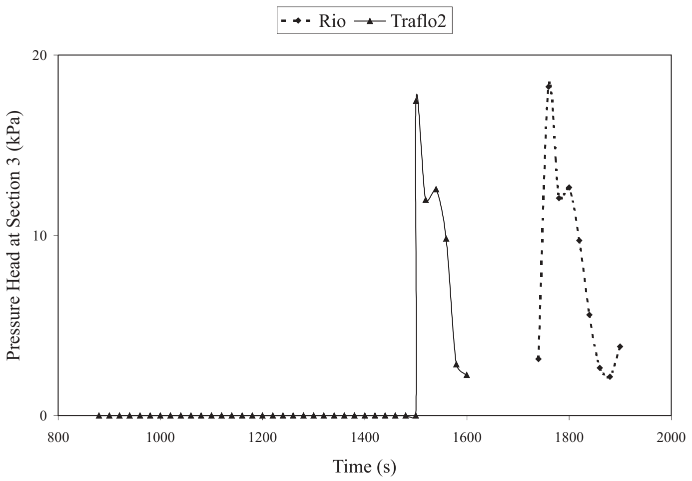

Fig. 11. Comparison Rio/Traflo 2.

ants successfully applied to the two case studies. The first was based on laboratory data and the second on field data. Agreement was found between predicted and measured values. During phase 2 and 4, the surge front location and propagation may easily be processed by the present model, which is also able to take into account the bore presence.

According to the numerical simulations, Traflo3 did not improve on the transient results obtained from Traflo1 and Traflo2. Because it is inordinately time consuming, the Traflo3 variant should be used only when the storm drainage system has an extremely dynamic transient flow behaviour. Pressure peak values are reached only at the moment the surge front arrives at the downstream (or upstream) boundary-end.

Further work should be done with more than one surge front to determine the trapped air bubble volume and the interaction between air flow and (water) transient flow. This and the air releases associated with air bubbles should be investigated concurrently. Also *in situ* data referring to flows varying rapidly are necessary to improve the Traflo3 model.

List of symbols

A	wetted cross-sectional area
a	waterhammer celerity
B	water surface width
B_r	weir width
c	gravity wave celerity
c_d	discharge coefficient
D	pipe diameter
f	Darcy friction coefficient
g	acceleration due to gravity
h	pressure head
h_L	energy head loss
h_0^*	weir height
L	pipe length
n	Manning friction coefficient
Q	discharge
Re	Reynolds number
S	friction slope
S_0	pipe (sewer) bottom slope
t	instantaneous time
V	mean cross-sectional velocity
w	interface (surge front) propagation velocity
x_1	length of pressurised flow zone
y	water depth
$\overline{y}$	distance from free – surface to the wetted cross – section centroid.

List of references

CANOE 1999, Urban hydrology software: User Manual, Sogreah-Alison-Insa, (Web site http://www.enpc.fr/cereve/HomePages/tassin/hydurb00/projet/doc_canoe/doccanoe.pdf) France.

CHAUDHRY, M. H. (1987), Applied hydraulic transient, Van Nostrand Reinhold Company, New York.

CHAUDHRY, M. H. (1993), Open-channel flow, Prentice Hall, New Jersey.

CUNGE, J.A. (1966), Comparison of physical and mathematical model test results on translation waves in the Oraison-Manosque power canal. La Houille Blanche, **22(1)**, 55-69 (in French).

CUNGE, J.A. and WEGNER M. (1966), Numerical integration of Barré de Saint-Venant's flow equations by means of an implicit scheme of finite differences. Applications in the case of alternately free and pressurized flow in a tunnel. La Houille Blanche, **22(1)**, 33-39 (in French).

CUNGE, J.A., HOLLY, F.M., JR. and VERWEY, A. (1980), Pratical aspects of computational river hydraulics, Pitman advanced publishing program, Boston.

FUAMBA, M. (1996), Experimental study on positive surge front in transient flow, Proc. 7th Int. Conf. on Pressure Surges and Fluid Transients in Pipelines and Open Channels, Harrogate, UK, BHR Group Ltd, 631-638.

FUAMBA, M. (1997), Modelling transient flow in sewer system, PhD. thesis, Katholieke Universiteit Leuven, Leuven, Belgium, 27-38 (in French).

HYDROWORKS (2000), Wastewater network simulation and analysis software: On-line documentation, (Web site http://www.wallingfordsoftware.com/products/hydroworks.asp) Wallingford Software Ltd. Oxfordshire, U.K.

JUN, B.H. (1985), Dynamic wave simulation of unsteady open channel and surcharge flows in sewer networks, PhD. thesis, University of Illinois at Urbana-Champaign, Ann Arbor, Michigan.

LI, J. and MCCORQUODALE, J.A. (1999), Modeling mixed flow in storm sewers, Journal of Hydraulic Engineering, ASCE, **125(11)**, 1170-1180.

MCCORQUODALE, J.A., and HAMAM, M.A. (1983), Modelling surcharged flow in sewers, Proc. Int. Symp. On Urban Hydrol., Hydr. And Sediment Control, University of Kentucky, Lexington, Ky., 331-338.

MEYER-PETER, E. and FAVRE, H. (1932), Ueber die Eigenschaften von Schwällen und die Berechnung von Unterwasserstollen. Schweizerische Bauzeitung, **100(4/5)**, 43-50.

MOUSE (2000), Professional engineering software: Reference manual, Danish Hydraulic Institute DHI Water & Environment, (Web site http://www.dhisoftware.com/mouse) Hørsholm, Denmark.

Rio (1993), Sewer system analysis program: Reference manual, Laboratorium voor Hydraulica, K.U. Leuven, Belgium, 1-69.

Roberson, J.A., Cassidy, J.J. and Chaudhry, M.H. (1998), Hydraulic engineering (Second edition), John Wiley & Sons, Inc., New York.

Song, C.S.S., Cardle, J.A. and Leung, K.S. (1983), Transient mixed-flow models for storm sewers, Journal of Hydraulic Engineering, ASCE, **109(11)**, 1487-1503.

Streeter, V.L. and Wylie, B.E. (1981), Fluid transients, Mc Graw-Hill Inc., New York.

Whitham, D.B. (1973), Linear and nonlinear waves, John Wiley & Sons, New York.

Wiggert, D.C. (1972), Transient flow in free-surface, pressurized systems, Journal of the Hydraulics Division, ASCE, **98(1)**, 11-27.

Yen, B.C. (1986), Hydraulics of sewers, Advances in Hydroscience, Vol. 14, Academic Press, Florida.